

Article

Metal-Templated Design: Enantioselective Hydrogen-Bond-Driven Catalysis Requiring Only Parts-per-Million Catalyst Loading

Weici Xu, Marcus Arieno, Henrik Löw, Kaifang Huang, Xiulan Xie, Thomas Cruchter, Qiao Ma, Jianwei Xi, Biao Huang, Olaf Wiest, Lei Gong, and Eric Meggers

J. Am. Chem. Soc., **Just Accepted Manuscript** • DOI: 10.1021/jacs.6b02769 • Publication Date (Web): 23 Jun 2016

Downloaded from <http://pubs.acs.org> on June 24, 2016

Just Accepted

“Just Accepted” manuscripts have been peer-reviewed and accepted for publication. They are posted online prior to technical editing, formatting for publication and author proofing. The American Chemical Society provides “Just Accepted” as a free service to the research community to expedite the dissemination of scientific material as soon as possible after acceptance. “Just Accepted” manuscripts appear in full in PDF format accompanied by an HTML abstract. “Just Accepted” manuscripts have been fully peer reviewed, but should not be considered the official version of record. They are accessible to all readers and citable by the Digital Object Identifier (DOI®). “Just Accepted” is an optional service offered to authors. Therefore, the “Just Accepted” Web site may not include all articles that will be published in the journal. After a manuscript is technically edited and formatted, it will be removed from the “Just Accepted” Web site and published as an ASAP article. Note that technical editing may introduce minor changes to the manuscript text and/or graphics which could affect content, and all legal disclaimers and ethical guidelines that apply to the journal pertain. ACS cannot be held responsible for errors or consequences arising from the use of information contained in these “Just Accepted” manuscripts.



1 **Metal-Templated Design: Enantioselective Hydrogen-Bond-Driven Catalysis**
2
3
4 **Requiring Only Parts-per-Million Catalyst Loading**
5
6
7

8 Weici Xu,¹ Marcus Arieno,² Henrik Löw,³ Kaifang Huang,¹ Xiulan Xie,³ Thomas Cruchter,³ Qiao
9 Ma,¹ Jianwei Xi,¹ Biao Huang,¹ Olaf Wiest,^{2,4*} Lei Gong,^{1*} and Eric Meggers^{1,3*}
10
11
12
13

14
15 ¹College of Chemistry and Chemical Engineering, Xiamen University, Xiamen 361005, People's
16 Republic of China
17
18
19

20 ²Department of Chemistry and Biochemistry, University of Notre Dame, Notre Dame, Indiana 46556,
21 USA
22
23
24

25 ³Fachbereich Chemie, Philipps-Universität Marburg, Hans-Meerwein-Strasse 4, 35043 Marburg,
26 Germany
27
28
29

30 ⁴Laboratory of Computational Chemistry and Drug Discovery, Laboratory of Chemical Genomics,
31 Peking University Shenzhen Graduate School, Shenzhen 518055, People's Republic of China
32
33
34
35

36
37
38
39 *Corresponding authors: owiest@nd.edu, gongl@xmu.edu.cn, meggers@chemie.uni-marburg.de
40
41
42
43
44
45
46
47
48
49
50
51
52
53
54
55
56
57
58
59
60

1 **Abstract:** Based on a metal-templated approach using a rigid and globular structural scaffold in the
2
3 form of a bis-cyclometalated octahedral iridium complex, an exceptionally active hydrogen-bond-
4 mediated asymmetric catalyst was developed and its mode of action investigated by crystallography,
5
6 NMR, computation, kinetic experiments, comparison with a rhodium congener, and reactions in the
7
8 presence of competing H-bond donors and acceptors. Relying exclusively on weak forces, the
9
10 enantioselective conjugate reduction of nitroalkenes can be executed at catalyst loadings as low as
11
12 0.004 mol% (40 ppm), representing turnover numbers of up to 20250. A rate acceleration by the
13
14 catalyst of 2.5×10^5 was determined. The origin of the catalysis is traced to an effective stabilization
15
16 of developing charges in the transition state by carefully orchestrated hydrogen bond and van der
17
18 Waals interactions between catalyst and substrates. This study demonstrates that the proficiency of
19
20 asymmetric catalysis merely driven by hydrogen bond and van der Waals interactions can rival
21
22 traditional activation through direct transition metal coordination of the substrate.
23
24
25
26
27
28
29
30
31
32
33
34
35
36
37
38
39
40
41
42
43
44
45
46
47
48
49
50
51
52
53
54
55
56
57
58
59
60

Introduction

Asymmetric catalysis is considered as one of the most efficient and economical strategies to access single enantiomers of a chiral molecule since only substoichiometric quantities of the chiral catalyst are required and remarkable progress has been made with respect to combining high asymmetric induction with low catalyst loadings. For example, employing a chiral iridium catalyst, Zhou and coworkers achieved a turnover number (TON) of 4550000 with an enantioselectivity of 98% ee for the enantioselective hydrogenation of acetophenone.^{1,2} Over the past 10-15 years, chiral organic compounds have complemented chiral transition metal complexes as powerful asymmetric catalysts.³ In one appealing mode of activation, which somewhat mimics enzymatic catalysis, weak forces such as hydrogen bond formation and van der Waals interactions are exploited to provide both the required rate acceleration as well as asymmetric induction.^{4,5} This mild mode of activation is very attractive because it ensures a high functional group tolerance. However, this comes at the cost of achieving high turnover numbers with catalyst loadings of 5-30% (≤ 20 TON) being still standard.⁶ A notable exception was recently reported by Song and coworkers for the desilylative kinetic resolution of racemic alcohols using extremely low catalyst loadings down to 0.0001 mol% (up to 440000 TON).⁷ The same group also demonstrated an acceleration of hydrogen bond catalysis on water allowing to reduce the catalyst loading for an enantioselective Michael addition to 0.01 mol% (up to 10000 TON).⁸

Nature solves this problem by steering multiple attractive weak interactions between enzyme catalyst and substrate in a cooperative fashion, thereby lowering the activation barrier through substrate proximity and electronic activation. This concept has been applied to the design of bi- and multifunctional catalysts.^{5,9} The activation of both the nucleophile and electrophile within a single catalyst provides the opportunity to achieve high catalytic activity and high asymmetric induction through a synergistic electronic activation of the involved substrates together with a control of their topological arrangement at the active site of the catalyst. However, getting the most out of this concept poses significant challenges. Firstly, finding the ideal position and orientation of the multiple functional groups involved in substrate binding and activation is not trivial and requires a versatile

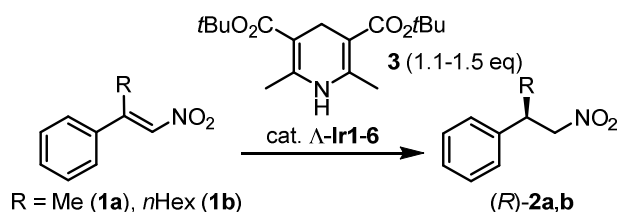
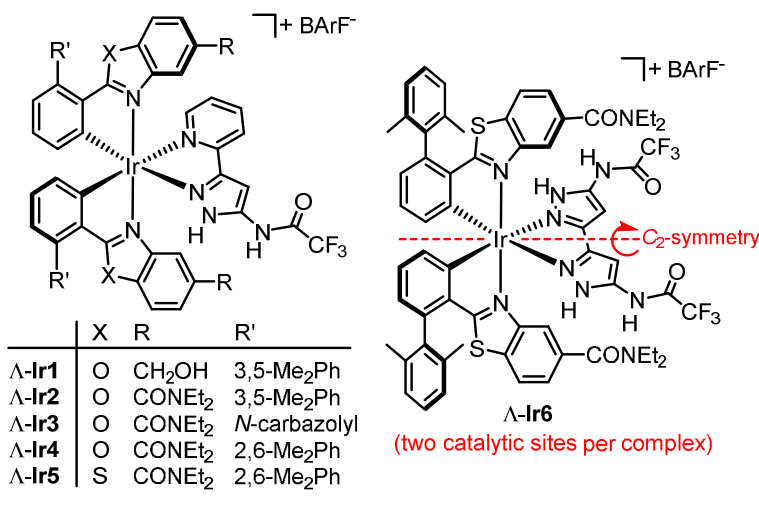
1 structural scaffold. Secondly, in cases where only weak forces are at play between the catalyst and the
2 substrates, entropy must play an important role because the highly ordered ternary complex out of the
3 two substrates and the catalyst only holds together by weak forces. These two points can rationalize
4 the often high catalyst loadings that are required by bifunctional thiourea catalysts.⁵
5
6
7
8
9

10 In this proof of principle study we demonstrate that a fine-tuned cooperativity of hydrogen
11 bond formation and van der Waals interactions implemented within a rigid template can provide an
12 extremely active multifunctional asymmetric catalyst achieving remarkable rate accelerations of
13 $k_{\text{cat}}/k_{\text{uncat}} = 2.5 \times 10^5$ with catalyst loadings down to 0.004 mol% and up to 20250 TON while retaining
14 high enantioselectivity (>90% ee).
15
16
17
18
19
20
21
22
23
24

25 Results and Discussion

26
27
28 **Catalyst Development.** We started this study with Λ -**Ir1**,¹⁰ a previously developed metal-
29 templated catalyst containing a structural iridium(III) center,^{11,12} which was reported to be an effective
30 asymmetric transfer hydrogenation catalyst. Here, the stereochemical information is provided by the
31 chiral-at-metal iridium, which also positions the catalytic functional group in a precise fashion using is
32 octahedral coordination environment. However, its performance diminishes at low catalyst loadings.
33 For example, at a catalyst loading of 0.1 mol%, the conjugate reduction of (*E*)-2-methyl-1-nitrostyrene
34 (**1a**) to the corresponding nitroalkane (*R*)-**2a** employing the Hantzsch ester **3** as the reducing agent
35 proceeds sluggishly with an incomplete conversion in the optimal solvent toluene at 20 °C and a low
36 enantioselectivity of 65% ee (Table 1, entry 1).¹³⁻¹⁵ An iterative improvement of this catalyst was
37 accomplished by replacing the hydroxyl groups with the stronger hydrogen bond acceptor *N,N*-
38 diethylcarboxamide (Λ -**Ir2**, entry 2),¹⁶⁻¹⁸ optimizing the substituent at the metalated phenyl moiety
39 (Λ -**Ir3** and Λ -**Ir4**, entries 3-6),¹⁶ replacing the benzoxazole ligands against benzothiazoles (Λ -**Ir5**,
40 entry 7), and by exchanging the pyridylpyrazole ligand with a bis-pyrazole (Λ -**Ir6**, entries 8-13). Note
41 that the final catalyst Λ -**Ir6** is C_2 -symmetrical and therefore contains two catalytic sites per iridium
42
43
44
45
46
47
48
49
50
51
52
53
54
55
56
57
58
59
60

1 complex. Λ -**Ir6** displays an astonishing activity, catalyzing the reaction **1a** \rightarrow (*R*)-**2a** with a loading of
2 only 0.01 mol% while maintaining a high enantioselectivity of 94% ee (entry 9). Using the substrate
3 (*E*)-2-*n*-hexyl-1-nitrostyrene (**1b**), a further reduced catalyst loading of 0.005 mol% is sufficient to
4 achieve a satisfactory enantioselectivity of 91% ee (entry 11).¹⁹ Relevant for aspects of sustainable
5 chemistry, this reaction can be executed completely devoid of any solvent, even resulting in improved
6 enantioselectivity.²⁰ For example, substrate **1b** is converted into (*R*)-**2b** using 0.005 mol% or 0.004
7 mol% Λ -**Ir6** with a 94% or 91% ee, respectively (entries 12 and 13). A catalyst loading of 0.004
8 mol% relates to a substrate/catalyst ratio of 25000 and 20250 TON for a conversion of 81% (entry
9 13).
10
11
12
13
14
15
16
17
18
19
20
21
22
23
24
25
26
27
28
29
30
31
32
33
34
35
36
37
38
39
40
41
42
43
44
45
46
47
48
49
50
51
52
53
54
55
56
57
58
59
60

Table 1. Ultra low-loading H-bond catalyst development.^a

entry	cat	mol% ^b	TON ^c	R	conditions ^d	<i>t</i> (h)	conv (%) ^e	ee (%) ^f
1	Δ -Ir1	0.1	470	Me	toluene, 20 °C	96	47	65
2	Δ -Ir2	0.1	990	Me	toluene, 20 °C	48	99	93
3	Δ -Ir3	0.1	980	Me	toluene, 20 °C	23	98	98
4	Δ -Ir3	0.05	1120	Me	toluene, 20 °C	24	56	94
5	Δ -Ir4	0.05	1880	Me	toluene, 20 °C	15	94	98
6	Δ -Ir4	0.02	2800	Me	toluene, 20 °C	22	56	94
7	Δ -Ir5	0.02	3200	Me	toluene, 20 °C	22	64	95
8	Δ -Ir6	0.02	4600	Me	toluene, 20 °C	22	92	97
9	Δ -Ir6	0.01	8600	Me	toluene, 20 °C	48	86	94
10	Δ -Ir6	0.01	8800	<i>n</i> Hex	toluene, 20 °C	24	88	96
11	Δ -Ir6	0.005	19400	<i>n</i> Hex	toluene, 40 °C	40	97	91
12	Δ -Ir6	0.005	18000	<i>n</i> Hex	no solvent, rt	48	90	94
13	Δ -Ir6	0.004	20250	<i>n</i> Hex	no solvent, rt	48	81	91

^a BArF = tetrakis[(3,5-di-trifluoromethyl)phenyl]borate. ^b Catalyst loadings provided in mol%. ^c Calculated turnover numbers. ^d Conditions: In anhydrous toluene under stirring with 1.5 eq. **3** (entries 1-11) or solvent-free in a ball mill with 1.1 eq. **3** (entries 12 and 13). ^e Conversion determined by ¹H-NMR. ^f Enantiomeric excess determined by chiral HPLC.

Substrate Scope and Gram Scale Reactions. As demonstrated by the results in Figure 1, catalyst Λ -**Ir6** displays an excellent substrate scope and provides for a broad range of β,β -disubstituted nitroalkenes ee values between 91 and 98% at catalyst loadings between 0.005 and 0.05 mol%. It is also worth noting that the reaction is readily scalable. For example, upon increasing the scale from milligram to gram scale, the catalytic performance of Λ -**Ir6** even increased slightly: Dissolved in 13 mL of toluene, 3.0 mg of Λ -**Ir6** (0.005 mol%) converted 6.2 g of **1b** into 6.1 g of (*R*)-**2b** with a high yield of 97% and 92% ee which relates to a TON of 19400 (Figure 1). Under solvent-free conditions, on a gram scale, a yield of 93% with 94% ee was observed (18600 TON).

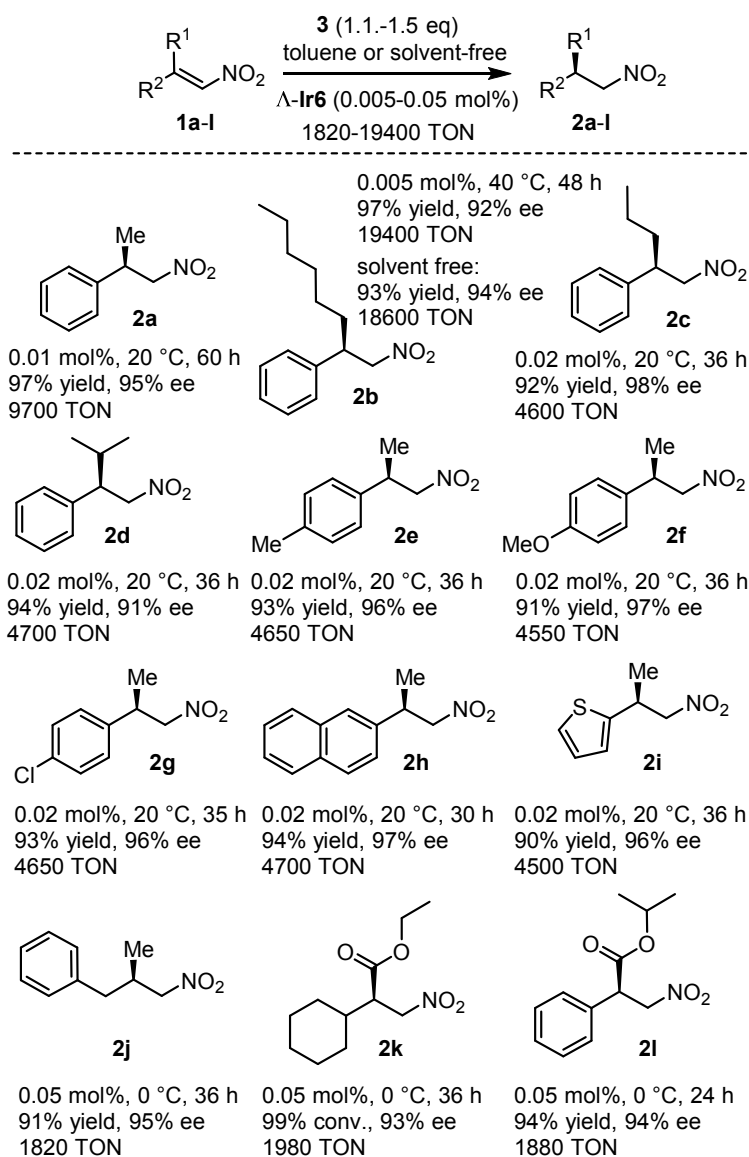


Figure 1. Substrate scope of the enantioselective transfer hydrogenation with Λ -**Ir6**.

1 **Excluding Direct Metal Involvement.** The surprisingly high catalytic activity of the
2
3 developed catalysts warrants a confirmation of the role of the involved transition metal, which was
4
5 addressed by two sets of experiments using the example of Λ -**Ir4**. Firstly, performed with 0.1 mol%
6
7 of Λ -**Ir4**, the catalyst was reisolated after each catalytic reaction (**1a** \rightarrow **2a**) in high yields and reused
8
9 multiple times without any significant loss of catalytic performance, thereby demonstrating its high
10
11 constitutional and configurational stability (Figure 2). Secondly, replacing the central iridium in Λ -**Ir4**
12
13 for the lighter congener rhodium provides a catalyst (Λ -**Rh4**) with almost indistinguishable catalytic
14
15 activity (Figure 3a), which can be traced back to highly similar coordination geometries of rhodium
16
17 and iridium as demonstrated by crystal structures of the bis-cyclometalated “core complexes” (Figure
18
19 3b) in which the coordinative bonds to iridium and rhodium vary only in a range from 0.005-0.025 Å.
20
21 Thus, the high inertness of the employed bis-cyclometalated iridium(III) complexes together with the
22
23 demonstrated insensitivity towards swapping the central metal precludes a direct involvement of the
24
25 metal in the catalytic mechanism and confirms that the metal exerts a purely structural role by
26
27 providing the essential chirality and serving as a central component of the structural scaffold.²¹
28
29 Furthermore, the observation that the catalyst can be reisolated and reused multiple times without
30
31 significantly affecting its catalytic performance reveals the constitutional and configurational stability
32
33 of the bis-cyclometalated organometallic complex, which is a prerequisite for achieving high turnover
34
35 numbers.
36
37
38
39
40
41
42
43
44
45
46
47
48
49
50
51
52
53
54
55
56
57
58
59
60

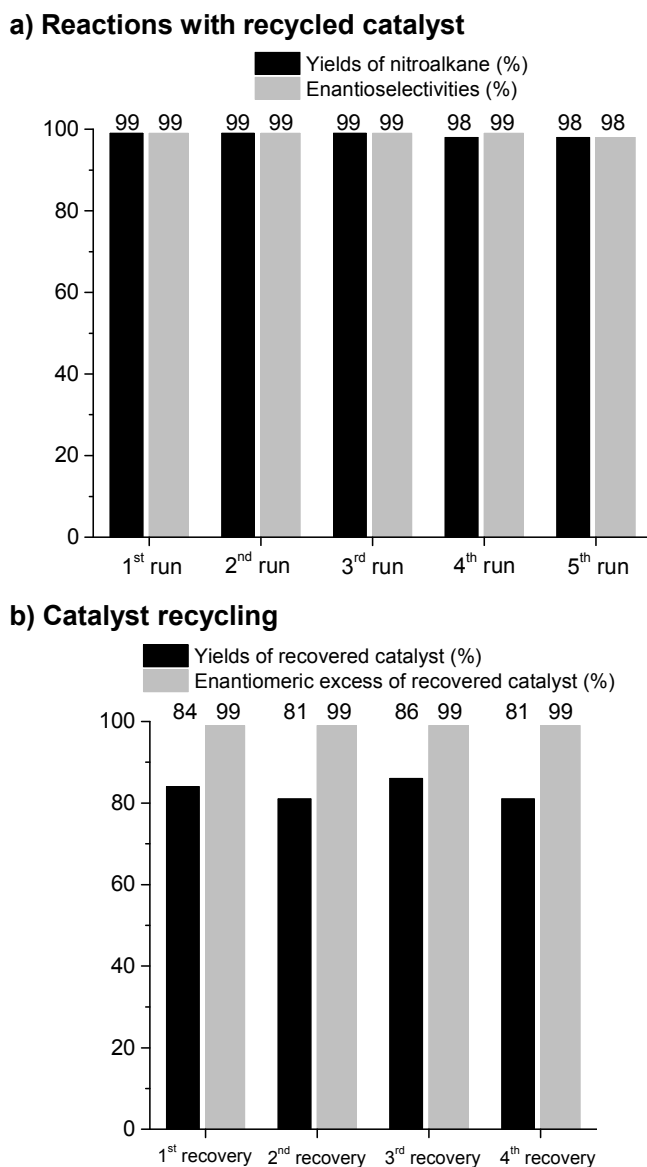


Figure 2. Catalyst recycling experiments with catalyst Λ -**Ir4** (0.1 mol%) for the conversion **1a** \rightarrow **2a**.

(a) Catalytic performance of recycled catalyst. (b) Yields and enantiopurities of the recovered catalyst after each reaction. Enantiomeric excess of recovered Λ -**Ir4** was determined by HPLC on a chiral stationary phase.

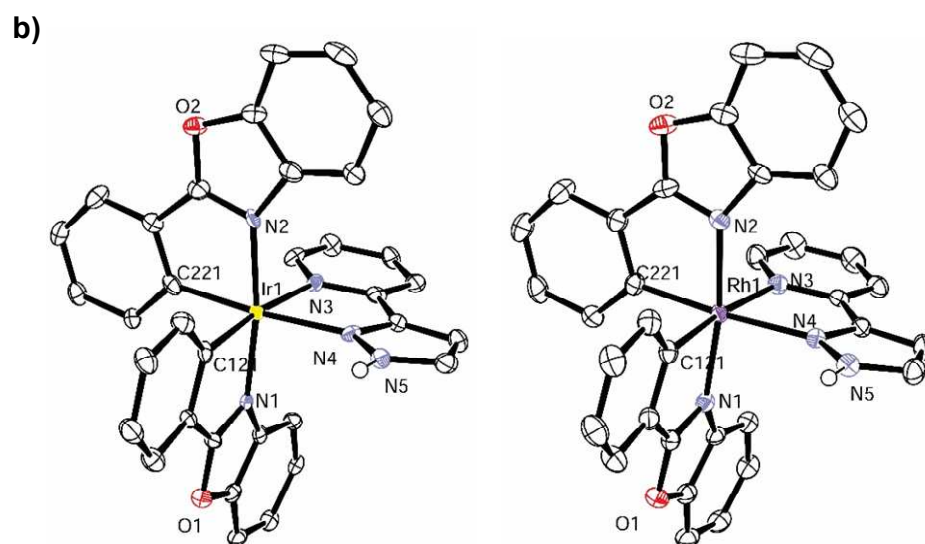
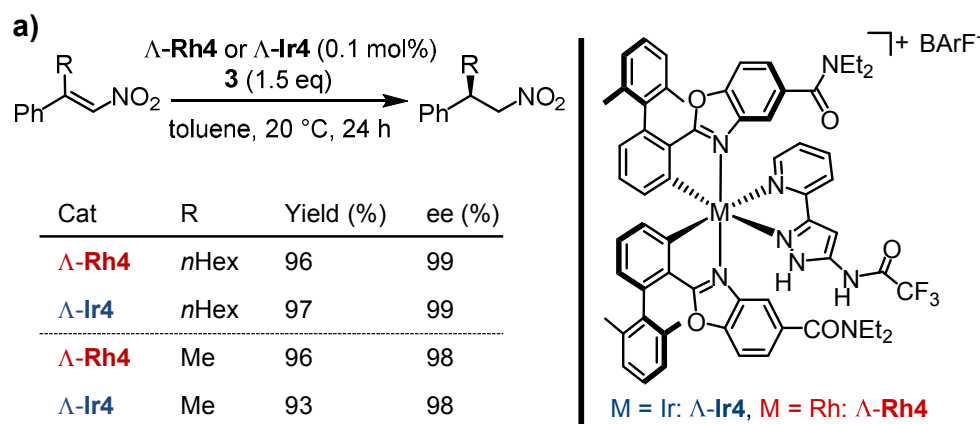


Figure 3. Comparison of homologous iridium and rhodium catalysts. (a) Conjugate reduction catalyzed by Δ -Ir4 and the lighter congener of Δ -Rh4. (b) X-ray crystal structures of the corresponding iridium and rhodium “core complexes” *rac*-Ir7 (CCDC no. 1460846) and *rac*-Rh7 (CCDC no. 1460844) with the bidentate ligands devoid of any substituents. ORTEP drawings with 50% thermal ellipsoids. The complexes were crystallized as their racemates but only the Δ -enantiomers are shown. The chloride counterions and solvent molecules are omitted for clarity. Distances of coordinative bonds (Å): Ir1-N1 = 2.045, Rh1-N1 = 2.040, Ir1-N2 = 2.050, Rh1-N2 = 2.042, Ir1-N3 = 2.141, Rh1-N3 = 2.164, Ir1-N4 = 2.113, Rh1-N4 = 2.138, Ir1-C121 = 2.028, Rh1-C121 = 2.012, Ir1-C221 = 2.035, Rh1-C221 = 2.013.

1 **Probing Hydrogen Bond Interactions.** Having confirmed the absence of any direct metal
2
3 coordination to a substrate, we next experimentally probed the involvement of hydrogen bonds during
4
5 catalysis. Firstly, the expected hydrogen bond driven mechanism is consistent with an observed high
6
7 sensitivity of the catalytic reaction towards competing hydrogen bond donors and acceptors. For
8
9 example, the addition of just one equivalent of ethanol or *N,N*-dimethylacetamide significantly slowed
10
11 down the reaction rate with dramatic declines in enantioselectivities to 20% and 8% ee (conversion **1a**
12
13 → (*R*)-**2a** with 0.02 mol% Λ -**Ir6**), respectively, while the presence of nitrobenzene decreased the
14
15 reaction rate significantly (66% instead of 92% conversion after 22 h), apparently by competing with
16
17 the substrate for the double hydrogen bond binding site at the catalyst (see Supporting Information for
18
19 more details). Secondly, the expected double hydrogen bond between catalyst and nitroalkene lends
20
21 further support from temperature dependent downfield chemical shifts of the N-H groups of simplified
22
23 model catalysts in the presence of a nitroalkene substrate (see Supporting Information for more
24
25 details). Thirdly, a co-crystal structure between a simplified model catalyst and a carboxylate
26
27 (trifluoroacetate), employed as a structural analog of a nitro compound displays the expected
28
29 association of the carboxylate substrate at the catalytic side (Figure 4). In this context it is worth
30
31 noting that Λ -**Ir6** represents only a weak Brønsted acid ($pK_a = 13$ in MeCN) and, for example, is not
32
33 capable of protonating the weak base pyridine in MeCN (see Supporting Information). A proton
34
35 transfer to the nitroalkene substrate in a pre-equilibrium can therefore be excluded, thus classifying
36
37 the mechanism as a real hydrogen bond mediated catalysis (general acid catalysis) and being clearly
38
39 distinct from typical Brønsted acid catalysis (specific acid catalysis).
40
41
42
43
44
45
46
47
48
49
50
51
52
53
54
55
56
57
58
59
60

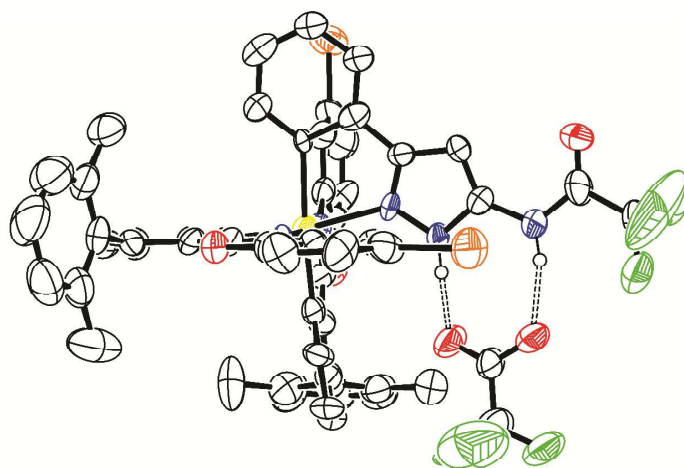


Figure 4. Co-crystal structure showing a double hydrogen bond interaction between a simplified model iridium complex (*rac*-**Ir8**) and a trifluoroacetate anion used as a structural analog of a nitro substrate (CCDC no. 1420596). ORTEP drawings with 50% probability thermal ellipsoids.

Probing Van der Waals Interactions. We next probed weak, non-covalent interactions between the nitroalkene substrate and the catalyst beyond hydrogen bond formation. This was accomplished by employing $^1\text{H-NMR}$ titration experiments to determine K_d values for the interaction of the nitroalkene **1a** with simplified model catalysts which only differ in their aromatic moiety (position R' in Table 1) (see Supporting Information for more details). As a result, K_d values decrease in the direction $R' = \text{H} > 3,5\text{-Me}_2\text{Ph} > 2,6\text{-Me}_2\text{Ph}$, which means that with increasing steric hindrance the binding affinity improves. Since the hydrogen bond formation of all three model catalysts is identical, this trend is indicative of attractive van der Waals interactions between the moiety R' and the nitroalkene substrate. Indeed, the co-crystal structure displayed in Figure 4 reveals how close one methyl group of the 2,6- Me_2Ph moiety comes to the nitroalkene substrate. These results are consistent with the observed trend in catalyst performance $\Lambda\text{-Ir4}$ ($R' = 2,6\text{-Me}_2\text{Ph}$) $>$ $\Lambda\text{-Ir2}$ ($R' = 3,5\text{-Me}_2\text{Ph}$), thus supporting our interpretation that our optimized catalyst achieves maximum binding affinity to the nitroalkene substrate through a combination out of hydrogen bond and van der Waals interactions. The aromatic and aliphatic moieties of the catalyst ligand sphere generate a hydrophobic cavity, which

1 can also be seen in the space filling model of Λ -**Ir6** (Figure 5d) and the model crystal structure in
2
3
4 Figure 4. Since nitro groups are only weak hydrogen bond acceptors,²² the additional van der Waals
5
6 interactions are apparently crucial for increasing the binding affinity for the nitroalkene substrate,
7
8 thereby being a prerequisite for a sufficient turnover at very low catalyst loadings.
9

10
11 **Kinetics.** The reaction rate is an important parameter for achieving a sufficient turnover
12
13 frequency at very low catalyst loadings. To determine the rate acceleration achieved by the catalyst Λ -
14
15 **Ir6**, we made use of the fact that Λ -**Ir6** displays an almost perfect asymmetric induction. For example,
16
17 at a catalyst loading of 0.2 mol% for the reaction **1b** \rightarrow (*R*)-**2b** an enantioselectivity of 99.3% ee is
18
19 obtained.²³ This means that the formation of the minor enantiomer at lower catalyst loadings must
20
21 arise from the uncatalyzed background reaction and therefore allows us to approximate the rate
22
23 acceleration of the Λ -**Ir6**-catalyzed (k_{cat}) versus uncatalyzed reaction (k_{uncat}) of $k_{\text{cat}}/k_{\text{uncat}} = 2.5 \times 10^5$.
24
25 Although such a rate acceleration cannot match the proficiency of enzyme catalysis, it is remarkable
26
27 for a small molecule catalyst that is limited to hydrogen bonding and van der Waals interactions.²⁴
28
29 The overall kinetic profile of this reaction, carried out under slightly diluted homogeneous conditions,
30
31 was determined to be first order with respect to each substrate and just 0.77 with respect to the catalyst
32
33 which is consistent with Λ -**Ir6** displaying two catalytic sites per complex. A determined ΔH^\ddagger of 34
34
35 kJ/mol and $-T\Delta S^\ddagger$ of 42 kJ/mol at 20 °C also demonstrates that the entropic penalty for reaching the
36
37 highly ordered ternary transition state outperforms the enthalpic part, being consistent with a highly
38
39 ordered ternary transition state that is only arranged by a combination of weak forces. This also
40
41 supports the notion that the limited flexibility of the employed metal template should be beneficial for
42
43 lowering the Gibbs free energy of activation (ΔG^\ddagger).
44
45
46
47
48
49

50 **Computational Study.** The overall catalyst design builds on extensive work of bifunctional
51
52 thiourea catalysis, including the asymmetric transfer hydrogenation of β,β -disubstituted nitroalkanes
53
54 with Hantzsch ester.^{5,14,15,25} The resulting hypothesis that the amidopyrazole moiety forms a double
55
56 hydrogen bond with the nitroalkene while a carboxamide moiety accepts a hydrogen bond from the
57
58
59
60

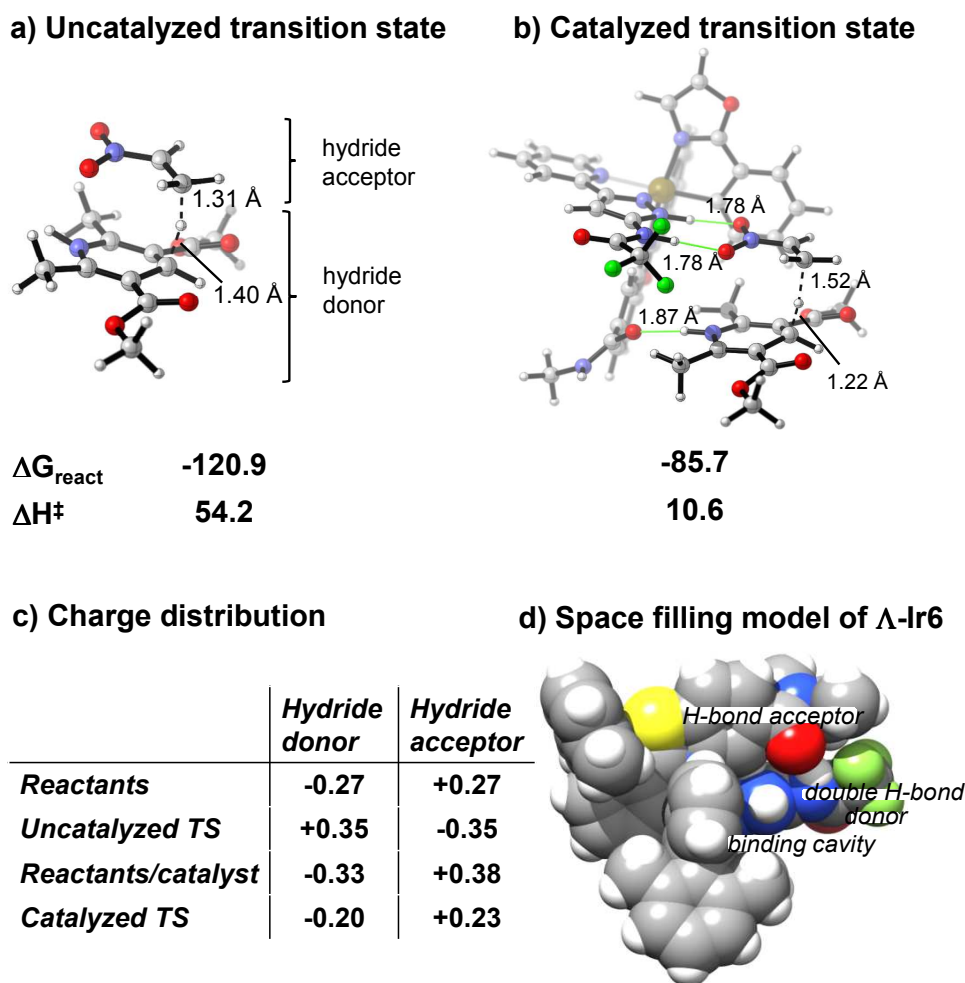
1 Hantzsch ester was probed using a computational study of the uncatalyzed and catalyzed reactions
2
3 summarized in Figure 5.
4

5
6 The calculated absolute activation enthalpy of 10.6 kJ/mol cannot be directly compared to the
7
8 experimental value 34 kJ/mol, due to the differences in the desolvation penalty for the catalyst and
9
10 substrates that is not included in the models calculated here. The difference in activation enthalpy
11
12 between the catalyzed and the uncatalyzed reaction of 43.6 kJ/mol is a better measure of the catalytic
13
14 effect and is in very good agreement with the experimentally observed rate acceleration of $k_{\text{cat}}/k_{\text{uncat}} =$
15
16 2.5×10^5 when using the value of ~ 5.5 kJ/mol for a tenfold acceleration at room temperature and
17
18 considering the differences in $\Delta\Delta S^\ddagger$ between reactions through a bimolecular and a termolecular
19
20 complex.²⁶ The calculated free energy of reaction is with -85.7 kJ/mol less exergonic in the catalyzed
21
22 compared to the uncatalyzed complex, where a value of -120.9 kJ/mol was obtained. The lower free
23
24 energy of reaction in the termolecular complex is due to the loss of the hydrogen bond between the
25
26 Hantzsch ester and the amide C=O as well as the π -stacking interactions that were responsible for the
27
28 assembly of the complex in the product.
29
30
31
32
33

34 Analysis of the geometry of the transition structures for the uncatalyzed and catalyzed reaction
35
36 shown in Figure 5a and 5b, respectively, reveals that the proposed hydrogen bonds in the catalyzed
37
38 reaction bring the two substrates into an orientation which perfectly resembles the preferred transition
39
40 structure of the uncatalyzed bimolecular reaction. The hydrogen bonds stabilizing the developing
41
42 charge in the transition structure are with 1.78 Å much shorter than the corresponding ones in the
43
44 reactant complex (1.93 Å) while the hydrogen bond holding the Hantzsch ester in place is with 1.87 Å
45
46 and 1.90 Å almost identical in the transition structure and reactant complex, respectively. The π -
47
48 systems of the nitroalkene and Hantzsch ester in the substrate complex are stacking against each other
49
50 and positioning them for the hydride transfer.
51
52
53
54

55 The differences in the lengths of the forming and breaking C-H bonds in the uncatalyzed and
56
57 catalyzed reaction point to substantial differences in the electronic character of the two transition
58
59 structures. While in the uncatalyzed reaction, the breaking C-H is with 1.40 Å slightly longer than the
60

1 forming one, the breaking C-H bond in the transition structure of the catalyzed reaction is with 1.22 Å
2
3 much shorter than the forming C-H bond. One approach to rationalize these differences is an analysis
4
5 of the partial charges (Figure 5c). In the uncatalyzed reaction, the partial charges of the hydride donor
6
7 and acceptor portions almost exactly flip, indicating a minimized charge buildup in the approximately
8
9 symmetric position of the hydrogen along the reaction coordinate. In contrast, the charge polarization
10
11 for the transition structure of the catalyzed reaction is similar but smaller, indicating that the
12
13 developing negative charge in the hydride acceptor portion of this early transition structure is
14
15 compensated by the strengthening hydrogen bonds. It should also be mentioned that the charge
16
17 analysis indicates an identical partial charge of +0.62 on the central metal in the reactant complex and
18
19 the transition structure, thus reemphasizing the structural rather than catalytic role of the metal. These
20
21 results are consistent with the hypothesis that the three hydrogen bonds induce a polarization that
22
23 increases the electrophilicity of the nitroalkene substrate as well as the hydride donor ability of the
24
25 Hantzsch ester in a highly pre-organized binding site shown in Figure 5d. This facilitates the hydride
26
27 transfer from the Hantzsch ester to the nitroalkene by stabilization of the developing charge in the
28
29 transition structure and is followed by a subsequent proton transfer to provide the final nitroalkane.
30
31
32
33
34
35
36
37
38
39
40
41
42
43
44
45
46
47
48
49
50
51
52
53
54
55
56
57
58
59
60



35
36
37
38
39
40
41
42
43
44
45
46
47
48
49
50
51
52

Figure 5. Computational investigations. (a,b) Comparison of the uncatalyzed and catalyzed transition structure of the hydrogenation, calculated at M06/6-311+G**+CPCM//6-31G* and M06/LANL2DZ/6-311+G**+CPCM//LANL2DZ/6-31G* levels of theory, respectively, for a model complex consisting of nitroethylene, Hantzsch ester bearing methyl instead *tert*-butyl esters, and a core structure derived from Δ -Ir4. (c) Charge distributions based on Mulliken charges at the γ -C of the Hantzsch ester (hydride donor) and the β -C of the nitroalkene (hydride acceptor). (d) CPK representation of the M06/LANL2DZ/6-31G* optimized structure of Δ -Ir6.

53 Conclusions

54
55
56
57
58
59
60

We here demonstrated the power of a metal-templated catalyst design by developing a hydrogen bond mediated asymmetric catalyst (Δ -Ir6) with remarkable performance, reaching

1 excellent yields and enantioselectivities at room temperature with turnover numbers as high as 20250
2
3 (0.004 mol% catalyst loading), which outperforms all reported organocatalysts and transition metal
4
5 catalysts for the conjugate reduction of β,β -disubstituted nitroalkenes for the reaction **1a** \rightarrow (*R*)- or
6
7 (*S*)-**2a**.^{14,27} This was accomplished by an iterative improvement of the catalyst through optimization of
8
9 hydrogen bond and van der Waals interactions with the involved substrates, limiting the
10
11 conformational flexibility of the catalyst, and by rendering the catalyst C_2 -symmetrical so that two
12
13 catalytic centers are operational per single iridium complex. The versatile globular geometry of the
14
15 employed octahedral scaffold gives a large freedom of a tailored arrangement of multiple functional
16
17 groups and is combined with a high degree of rigidity which reduces the entropic penalty of the
18
19 transition state and allows an acceleration of the asymmetric transfer hydrogenation $k_{\text{cat}}/k_{\text{uncat}} = 2.5 \times$
20
21 10^5 . Λ -**Ir6** apparently mimics somewhat the function of enzymes by perfectly orchestrating hydrogen
22
23 bond as well as van der Waals interactions with the substrates within a binding cleft, while
24
25 minimizing entropic effects due to a rigid, preorganized catalyst structure. Nitroalkanes are versatile
26
27 chiral building blocks and the application of these insights gained for the high performance catalytic
28
29 enantioselective conjugate reduction of β,β -disubstituted nitroalkenes to the Friedel-Crafts alkylation
30
31 of β,β -disubstituted nitroalkenes is ongoing in our laboratory.²⁸
32
33
34
35
36
37
38
39

40 Experimental Section

41 **Synthesis of enantiomerically pure catalysts.** All chiral-at-metal iridium complexes were
42
43 synthesized following a previously developed auxiliary-mediated strategy.^{10,29} The iridium complexes
44
45 Λ -**Ir1**,¹⁰ Λ -**Ir2**,^{16a} and Λ -**Ir3**^{16a} have been reported. The new catalysts Λ -**Ir4-6** were synthesized in a
46
47 more economical fashion by employing the readily available amino acid *L*-proline as the chiral
48
49 auxiliary.^{16b,30} The new rhodium complex Λ -**Rh4** was obtained by resolution of a racemic mixture on
50
51 HPLC using a chiral stationary phase. A detailed description of the synthesis and characterization of
52
53 these complexes is provided in the Supporting Information.
54
55
56
57
58
59
60

1 **Mechanistic investigations.** Experimental details of the mechanistic investigations, including
2
3 computation, NMR experiments, kinetics, and crystallographic experiments are provided in the
4
5 Supporting Information.
6
7

8 **Asymmetric transfer hydrogenations.** As a characteristic example for the reaction, to a
9
10 solution of catalyst Λ -**Ir6** (3.0 mg, 1.340 μ mol, 0.005 mol% catalyst loading) in freshly distilled
11
12 toluene (13.4 mL), nitroalkene **1b** (6.244 g, 26.80 mmol) and *tert*-butyl Hantzsch ester (9.120 g, 29.48
13
14 mmol) were added. The reaction was stirred at 40 °C for 48 hours under an atmosphere of argon.
15
16 After cooling to room temperature, the mixture was diluted with *n*-hexane and then directly subjected
17
18 to flash silica gel column chromatography with EtOAc/*n*-hexane (1:100 to 1:50) to afford the product
19
20 (*R*)-**2b** (6.085 g, 25.89 mmol, 97% yield) with 92% ee as determined by HPLC on a chiral stationary
21
22 phase. Complete experimental details of this and all other catalytic reactions are provided in the
23
24 Supporting Information.
25
26
27
28
29
30

31 **Supporting Information.** Synthetic details, details of mechanistic experiments, HPLC traces,
32
33 crystallographic data, computational study, and NMR study. This material is available free of charge
34
35 via the Internet at <http://pubs.acs.org>.
36
37
38
39

40 **Acknowledgments:**

41
42 We thank the National Natural Science Foundation of P. R. China (grant nos. 21272192, 21472154
43
44 and 21572184), the Program for Changjiang Scholars and Innovative Research Team of P. R. China
45
46 (PCSIRT), the National Thousand Talents Program of P. R. China, the Fundamental Research Funds
47
48 for the Central Universities (grant no. 20720160027), and the 985 Program of the Chemistry and
49
50 Chemical Engineering disciplines of Xiamen University.
51
52
53
54
55
56
57
58
59
60

References:

- 1 (a) For overviews on highly efficient transition metal catalyzed asymmetric hydrogenations, see:
- (a) Blaser, H.-U.; Pugin, B.; Spindler, F. *Top. Organomet. Chem.* **2012**, *42*, 65–102. (b) Arai, N.; Ohkuma, T. *Chem. Record* **2012**, *12*, 284–289. (c) Xie, J.-H. Bao, D.-H. Zhou, Q.-L. *Synthesis* **2015**, *47*, 460–471.
- 2 Xie, J.-H.; Liu, X.-Y.; Xie, J.-B.; Wang, L.-X.; Zhou, Q.-L. *Angew. Chem. Int. Ed.* **2011**, *50*, 7329–7332.
- 3 For recent reviews on asymmetric organocatalysis, see: (a) List, B.; Yang, J. W. *Science* **2006**, *313*, 1584–1586. (b) MacMillan, D. W. C. *Nature* **2008**, *455*, 304–308. (c) Wong, O. A.; Shi, Y. *Chem. Rev.* **2008**, *108*, 3958–3987. (d) Dondoni, A.; Massi, A. *Angew. Chem. Int. Ed.* **2008**, *47*, 4638–4660. (e) Denmark, S. E.; Beutner, G. L. *Angew. Chem. Int. Ed.* **2008**, *47*, 1560–1638. (f) Palomo, C.; Oiarbide, M.; López, R. *Chem. Soc. Rev.* **2009**, *38*, 632–653. (g) Brière, J.-F.; Oudeyer, S.; Dalla, V.; Levacher, V. *Chem. Soc. Rev.* **2012**, *41*, 1696–1707. (h) Pellissier, H. *Adv. Synth. Catal.* **2012**, *354*, 237–294. (i) Liu, T.; Xie, M.; Chen, Y. *Chem. Soc. Rev.* **2012**, *41*, 4101–4112. (j) Hernández, J. G.; Juaristi, E. *Chem. Commun.* **2012**, *48*, 5396–5409. (k) Mahlau, M.; List, B. *Angew. Chem. Int. Ed.* **2013**, *52*, 518–533. (l) Alemán, J.; Cabrera, S. *Chem. Soc. Rev.* **2013**, *42*, 774–793. (m) Wei, Y.; Shi, M. *Chem. Rev.* **2013**, *113*, 6659–6690. (n) Duan, J.; Li, P. *Catal. Sci. Technol.* **2014**, *4*, 311–320. (o) Fang, X.; Wang, C.-J. *Chem. Commun.* **2015**, *51*, 1185–1197. (p) Atodiresei, I.; Vila, C.; Rueping, M. *ACS Catal.* **2015**, *5*, 1972–1985.
- 4 For pioneering work on the generic use of asymmetric H-bonding catalysis, see: (a) Sigman, M. S.; Jacobsen, E. N. *J. Am. Chem. Soc.* **1998**, *120*, 4901–4902. (b) Sigman, M. S.; Vachal, P.; Jacobsen, E. N. *Angew. Chem. Int. Ed.* **2000**, *39*, 1279–1281. (c) Vachal, P.; Jacobsen, E. N. *Org. Lett.* **2000**, *2*, 867–870. (d) Vachal, P.; Jacobsen, E. N. *J. Am. Chem. Soc.* **2002**, *124*, 10012–10014.

- 1
2
3
4
5
6
7
8
9
10
11
12
13
14
15
16
17
18
19
20
21
22
23
24
25
26
27
28
29
30
31
32
33
34
35
36
37
38
39
40
41
42
43
44
45
46
47
48
49
50
51
52
53
54
55
56
57
58
59
60
- 5 (a) Schreiner, P. R. *Chem. Soc. Rev.* **2003**, *32*, 289–296. (b) Takemoto, Y. *Org. Biomol. Chem.* **2005**, *3*, 4299–4306. (c) Connon, S. J. *Chem. Eur. J.* **2006**, *12*, 5418–5427. (d) Doyle, A. G.; Jacobsen, E. N. *Chem. Rev.* **2007**, *107*, 5713–5743. (e) Yu, X.; Wang, W. *Chem. Asian J.* **2008**, *3*, 516–532. (f) Knowles, R. R.; Jacobsen, E. N. *Proc. Natl. Acad. Sci. USA* **2010**, *107*, 20678–20685. (g) Auvil, T. J.; Schafer, A. G.; Mattson, A. E. *Eur. J. Org. Chem.* **2014**, 2633–2646.
- 6 For a recent review on low-loading asymmetric organocatalysis, see: Giacalone, F.; Gruttadauria, M.; Agrigento, P.; Noto, R. *Chem. Soc. Rev.* **2012**, *41*, 2406–2447.
- 7 Park, S. Y.; Lee, J.-W.; Song, C. E. *Nat. Commun.* **2015**, *6*, 7512.
- 8 Bae, H. Y.; Song, C. E. *ACS Catal.* **2015**, *5*, 3613–3619.
- 9 (a) Sawamura, M.; Ito, Y. *Chem. Rev.* **1992**, *92*, 857–871. (b) Shibasaki, M.; Yoshikawa, N. *Chem. Rev.* **2002**, *102*, 2187–2210. (c) Kano, T.; Maruoka, K. *Chem. Commun.* **2008**, 5465–5473. (d) Liu, X.; Lin, L.; Feng, X. *Chem. Commun.* **2009**, 6145–6158. (e) Lu, L.; An, X.; Chen, J.; Xiao, W. *Synlett* **2012**, *23*, 490–508. (f) Stegbauer, L.; Sladojevich, F.; Dixon, D. J. *Chem. Sci.* **2012**, *3*, 942–958.
- 10 Chen, L.-A.; Xu, W.; Huang, B.; Ma, J.; Wang, L.; Xi, J.; Harms, K.; Gong, L.; Meggers, E. J. *Am. Chem. Soc.* **2013**, *135*, 10598–10601.
- 11 For reviews covering chiral-at-metal complexes in catalysis, see: (a) Brunner, H. *Angew. Chem. Int. Ed.* **1999**, *38*, 1194–1208. (b) Knight, P. D.; Scott, P. *Coord. Chem. Rev.* **2003**, *242*, 125–143. (c) Fontecave, M.; Hamelin, O.; Ménage, S. *Top. Organomet. Chem.* **2005**, *15*, 271–288. (d) Bauer, E. B. *Chem. Soc. Rev.* **2012**, *41*, 3153–3167. (e) Gong, L.; Chen, L.-A.; Meggers, E. *Angew. Chem. Int. Ed.* **2014**, *53*, 10868–10874. (f) Cao, Z.-Y.; Brittain, W. D. G.; Fossey, J. S.; Zhou, F. *Catal. Sci. Technol.* **2015**, *5*, 3441–3451.
- 12 For the design of metal-templated asymmetric catalysts from other groups, see: (a) Belokon, Y. N.; Bulychev, A. G.; Maleev, V. I.; North, M.; Malfanov, I. L.; Ikonnikov, N. S. *Mendeleev*

- 1 *Commun.* **2004**, *14*, 249–250. (b) Ganzmann, C.; Gladysz, J. A. *Chem. Eur. J.* **2008**, *14*, 5397–
2 5400. (c) Kurono, N.; Arai, K.; Uemura, M.; Ohkuma, T. *Angew. Chem. Int. Ed.* **2008**, *47*, 6643–
3 6646. (d) Belokon, Y. N.; Maleev, V. I.; North, M.; Larionov, V. A.; Savel'yeva, T. F.; Nijland,
4 A.; Nelyubina, Y. V. *ACS Catal.* **2013**, *3*, 1951–1955. (e) Maleev, V. I.; North, M.; Larionov, V.
5 A.; Fedyanin, I. V.; Savel'yeva, T. F.; Moscalenko, M. A.; Smolyakov, A. F.; Belokon, Y. N. *Adv.*
6 *Synth. Catal.* **2014**, *356*, 1803–1810. (f) Lewis, K. G.; Ghosh, S. K.; Bhuvanesh, N.; Gladysz, J.
7 A. *ACS Cent. Sci.* **2015**, *1*, 50–56. (g) Larionov, V. A.; Markelova, E. P.; Smol'yakov, A. F.;
8 Savel'yeva, T. F.; Maleev, V. I.; Belokon, Y. N. *RSC Adv.* **2015**, *5*, 72764–72771. (h) Serra-Pont,
9 A.; Alfonso, I.; Jimeno, C.; Solà, J. *Chem. Commun.* **2015**, *51*, 17386–17389. (i) Kumar, A.;
10 Ghosh, S. K.; Gladysz, J. A. *Org. Lett.* **2016**, *18*, 760–763. (j) Ghosh, S. K.; Ganzmann, C.;
11 Bhuvanesh, N.; Gladysz, J. A. *Angew. Chem. Int. Ed.* **2016**, *55*, 4356–4360.
- 12
13
14
15
16
17
18
19
20
21
22
23
24
25
26
27 13 For selected examples of organocatalytic asymmetric transfer hydrogenations with Hantzsch
28 ester, see: (a) Yang, J. W.; Hechavarría Fonseca, M. T.; List, B. *Angew. Chem. Int. Ed.* **2004**, *43*,
29 6660–6662. (b) Hoffmann, S.; Seayad, A. M.; List, B. *Angew. Chem. Int. Ed.* **2005**, *44*, 7424–
30 7427. (c) Kang, Q.; Zhao, Z.-A.; You, S.-L. *Adv. Synth. Catal.* **2007**, *349*, 1657–1660. (d) Kang,
31 Q.; Zhao, Z.-A.; You, S.-L. *Org. Lett.* **2008**, *10*, 2031–2034. (e) Han, Z.-Y.; Xiao, H.; Chen, X.-
32 H.; Gong, L.-Z. *J. Am. Chem. Soc.* **2009**, *131*, 9182–9183. (f) Zhang, Y.-C.; Zhao, J.-J.; Jiang, F.;
33 Sun, S.-B.; Shi, F. *Angew. Chem. Int. Ed.* **2014**, *53*, 13912–13915. (g) Wang, S.-G.; You, S.-L.
34 *Angew. Chem. Int. Ed.* **2014**, *53*, 2194–2197. (h) Cai, X.-F.; Guo, R.-N.; Feng, G.-S.; Wu, B.;
35 Zhou, Y.-G. *Org. Lett.* **2014**, *16*, 2680–2683. (i) Wang, Z.; Ai, F.; Wang, Z.; Zhao, W.; Zhu, G.;
36 Lin, Z.; Sun, J. *J. Am. Chem. Soc.* **2015**, *137*, 383–389. (j) Shugrue, C. R.; Miller, S. J. *Angew.*
37 *Chem. Int. Ed.* **2015**, *54*, 11173–11176.
- 38
39
40
41
42
43
44
45
46
47
48
49
50
51
52 14 For the organocatalytic asymmetric transfer hydrogenation of nitroalkenes, see: (a) Martin, N. J.
53 A.; Ozores, L.; List, B. *J. Am. Chem. Soc.* **2007**, *129*, 8976–8977. (b) Martin, N. J. A.; Cheng, X.;
54 List, B. *J. Am. Chem. Soc.* **2008**, *130*, 13862–13863. (c) Schneider, J. F.; Falk, F. C.; Fröhlich, R.;
55 Paradies, J. *Eur. J. Org. Chem.* **2010**, 2265–2269. (d) Schneider, J. F.; Lauber, M. B.; Muhr, V.;
56
57
58
59
60

- 1 Kratzer, D.; Paradies, J. *Org. Biomol. Chem.* **2011**, *9*, 4323–4327. (e) Anderson, J. C.; Koovits, P.
2
3 J. *Chem. Sci.* **2013**, *4*, 2897–2901. (f) Martinelli, E.; Vicini, A. C.; Mancinelli, M.; Mazzanti, A.;
4
5 Zani, P.; Bernardi, L.; Fochi, M. *Chem. Commun.* **2015**, *51*, 658–660. For a racemic version, see:
6
7 Zhang, Z.; Schreiner, P. *Synthesis* **2007**, 2559–2564.
8
9
10
11 15 For recent reviews on asymmetric transfer hydrogenation with Hantzsch ester, see: (a) You, S.-L.
12
13 *Chem. Asian J.* **2007**, *2*, 820–827. (b) Zheng, C.; You, S.-L. *Chem. Soc. Rev.* **2012**, *41*, 2498–
14
15 2518.
16
17
18 16 (a) Chen, L.-A.; Tang, X.; Xi, J.; Xu, W.; Gong, L.; Meggers, E. *Angew. Chem. Int. Ed.* **2013**, *52*,
19
20 14021–14025; (b) Liu, J.; Gong, L.; Meggers, E. *Tetrahedron Lett.* **2015**, *56*, 4653–4656.
21
22
23 17 For hydrogen-bond basicity and affinity scales, see: Laurence, C.; Brameld, K. A.; Graton, J.; Le
24
25 Questel, J.-Y.; Renault, E. *J. Med. Chem.* **2009**, *52*, 4073–4086.
26
27
28 18 For selected examples of carboxamides as proposed hydrogen bond acceptors in thiourea
29
30 catalysts, see: (a) Zuend, S. J.; Jacobsen, E. N. *J. Am. Chem. Soc.* **2009**, *131*, 15358–15374. (b)
31
32 Yeung, C. S.; Ziegler, R. E.; Porco, J. A.; Jacobsen, E. N. *J. Am. Chem. Soc.* **2014**, *136*, 13614–
33
34 13617.
35
36
37 19 Under our optimized reaction conditions, the reaction mixture is a suspension at the beginning
38
39 due to a limited solubility of the Hantzsch ester in toluene and becomes homogeneous over the
40
41 course of the reaction.
42
43
44 20 For hydrogen bond mediated catalysis under solvent-free conditions, see for example: (a) Wang,
45
46 Y.-F.; Chen, R.-X.; Wang, K.; Zhang, B.-B.; Li, Z.-B.; Xu, D.-Q. *Green Chem.* **2012**, *14*, 893–
47
48 895. (b) Jörres, M.; Mersmann, S.; Raabe, G.; Bolm, C. *Green Chem.* **2013**, *15*, 612–616.
49
50
51
52 21 These two different structural aspects of the metal can be illustrated with two straightforward
53
54 experiments: Firstly, as to be expected, Λ -**Ir4** and Δ -**Ir4** convert the substrate **1b** to the mirror
55
56 imaged products (*R*)-**2b** and (*S*)-**2b**, respectively. Secondly, the ligands alone, devoid of any
57
58
59
60

- 1 metal, not only provide the product in a racemic form but also possess an insignificant catalytic
2 activity. See Supporting Information for more details.
3
4
5
6
7 22 Laurence, C.; Graton, J.; Berthelot, M.; Besseau, F.; Le Questel, J.-Y.; Luçon, M.; Ouvrard, C.;
8 Planchat, A.; Renault, E. *J. Org. Chem.* **2010**, *75*, 4105–4123.
9
10
11
12 23 We did not observe any product racemization or decomposition so that the observed
13 enantioselectivities are a direct consequence of the degree of asymmetric induction and the
14 background reaction.
15
16
17
18
19 24 Zhang, X.; Houk, K. N. *Acc. Chem. Res.* **2005**, *38*, 379–385.
20
21
22 25 For an early example of the asymmetric activation of nitroalkenes with a bifunctional thiourea
23 catalyst, see: Okino, T.; Hoashi, Y.; Takemoto, Y. *J. Am. Chem. Soc.* **2003**, *125*, 12672–12673.
24
25
26
27 26 For an overview of the problems with a more quantitative estimate of the entropies of solvation
28 and activation, see for example: Plata, R. E.; Singleton, D. A. *J. Am. Chem. Soc.* **2015**, *137*,
29 3811–3826.
30
31
32
33
34
35 27 For metal-catalyzed asymmetric conjugate reductions of nitroalkenes, see: (a) Czekelius, C.;
36 Carreira, E. M. *Angew. Chem. Int. Ed.* **2003**, *42*, 4793–4795. (b) Czekelius, C.; Carreira, E. M.
37 *Org. Lett.* **2004**, *6*, 4575–4577. (c) Czekelius, C.; Carreira, E. M. *Org. Process Res. Dev.* **2007**,
38 *11*, 633–636. (d) Soltani, O.; Ariger, M. A.; Carreira, E. M. *Org. Lett.* **2009**, *11*, 4196–4198. (e)
39 Tang, Y.; Xiang, J.; Cun, L.; Wang, Y.; Zhu, J.; Liao, J.; Deng, J. *Tetrahedron: Asymmetry* **2010**,
40 *21*, 1900–1905. (f) Li, S.; Huang, K.; Cao, B.; Zhang, J.; Wu, W.; Zhang, X. *Angew. Chem. Int.*
41 *Ed.* **2012**, *51*, 8573–8576. (g) Zhao, Q.; Li, S.; Huang, K.; Wang, R.; Zhang, X. *Org. Lett.* **2013**,
42 *15*, 4014–4017. (h) Li, S.; Huang, K.; Zhang, J.; Wu, W.; Zhang, X. *Chem. Eur. J.* **2013**, *19*,
43 10840–10844. (i) Yu, Y.-B.; Cheng, L.; Li, Y.-P.; Fu, Y.; Zhu, S.-F.; Zhou, Q.-L. *Chem.*
44 *Commun.* **2016**, *52*, 4812–4815.
45
46
47
48
49
50
51
52
53
54
55
56
57
58
59
60

- 1
2
3
4
5
6
7
8
9
10
11
12
13
14
15
16
17
18
19
20
21
22
23
24
25
26
27
28 Nitro groups can undergo a variety of useful transformations. See: Berner, O. M.; Tedeschi, L.;
Enders, D. *Eur. J. Org. Chem.* **2002**, 1877–1894 (and references therein).
29 Helms, M.; Lin, Z.; Gong, L.; Harms, K.; Meggers, E. *Eur. J. Inorg. Chem.* **2013**, 4164–4172.
30 Helms, M.; Wang, C.; Orth, B.; Harms, K.; Meggers, E. *Eur. J. Inorg. Chem.* **2016**, DOI:
10.1002/ejic.201600260.

19
20
21
22
23
24
25
26
27
28
29
30
31
32
33
34
35
36
37
38
39
40
41
42
43
44
45
46
47
48
49
50
51
52
53
54
55
56
57
58
59
60

TOC graphic:

